

# Continuous Broadband MWP True-Time Delay with PbS-PMMA and -SU8 waveguides

Joaquin Perez, *Member IEEE*, Isaac Suarez, Javier Hervas, Amelia Lavinia Ricchiuti, Juan P. Martinez-Pastor and Salvador Sales, *Senior Member, IEEE*.

**Abstract**— A new microwave true-time delay (TTD) photonic unit based on the dispersion of PbS colloidal quantum dots (QDs) in a Polymethyl methacrylate (PMMA) and the SU8 photoresist is presented. With this aim, the PbS-PMMA and PbS-SU8 nanocomposites are integrated on a silicon platform in the form of a planar and ridge waveguides, respectively. When PbS QDs on those structures are pumped below their band-gap, a phase shift and a temporal delay in an optically conveyed (at 1550 nm) microwave signal is performed. The results of these devices show potential benefits over current TTD technologies, since the proposed photonic waveguide structures allows real-time adjustment of the temporal delay by tuning the power of the pumping signal, more than 3.5 ps over 25 GHz, and a high level of integration due to the novel proposed photonic waveguide structures and the materials used.

**Index Terms**— Integrated microwave photonics, nanocomposites, optical signal processing, colloidal quantum dots, optical delay lines, optical waveguide components

## I. INTRODUCTION

MICROWAVE photonics (MWP) [1] has emerged over the last decades as an exciting discipline based on the transportation and processing of microwave signals over optical carriers in order to carry out radiofrequency (RF) signal processing functions [2], [3]. MWP enables the broadband, interference-immune and low loss transport and processing of RF signals, together with the possibility of performing multiple applications that are complex or even impossible to carry out with traditional electrical approaches, improving the performances of broad range of fields, such as

Manuscript received by January 15, 2016, revised by April 18, and accepted by April 28, 2016. This work was supported in part by the Spanish MICINN through the project TEC2014-53727-C2-1-R, by the Research Excellency Award Program GVA PROMETEO 2013/012, PROMETEOII/2014/059 and by the EU-NAVOLCHI (project 288869). J. Hervas's work is supported by the Spanish MECD FPU scholarship (FPU13/04675), A. L. Ricchiuti's work is supported by the grant of the program SANTIAGO GRISOLÍA, and J. Perez's work is supported by Spanish MINECO Juan de la Cierva Fellowship JCI-2012-14805.

J. Perez, J. Hervas, A. L. Ricchiuti, and S. Sales are with the iTEAM Research Institute, Optical Quantum and Communications Group, Universidad Politécnic de Valencia, Valencia 46022, Spain (e-mail: joapeso@upv.es; jaherpe2@teleco.upv.es; amric1@upv.es, [ssales@dcom.upv.es](mailto:ssales@dcom.upv.es))

I. Suárez and J. Martínez-Pastor are with UMDO, Instituto de Ciencia de los Materiales, Universidad de Valencia, Valencia 46071, Spain (e-mail: isaac.suarez@uv.es; martinep@uv.es).

Copyright (c) 2016 IEEE. Personal use of this material is permitted. However, permission to use this material for any other purposes must be obtained from the IEEE by sending a request to [pubs-permissions@ieee.org](mailto:pubs-permissions@ieee.org)

wireless communications, radar, signal filtering or sensing [4]. Those applications are based on basic functions such as phase shifting (PS) or true-time delay (TTD) [5]. Therefore, MWP solutions let broadband operations and enhanced tunability on TTD and PSs for arbitrary waveform generation, tunable and reconfigurable filtering, optoelectronic oscillators or beam steering. Moreover, the MWP can be integrated in photonic integrated circuits (PICs), field known as integrated microwave photonics (IMWP), in order to provide additional advantages as compactness, easiness of reproducibility and limited costs [6].

In this way, one fundamental key block of several MWP functionalities, for example in tunable filtering, is the TTD device, useful to overcome limitations of the conventional electrical approximations, like frequency-dependent losses, or to enable ultra-wideband operations. Examples of photonics TTDs architectures are the use of optical fiber links along with a tunable laser to feed a phase array antenna system [7], the use of semiconductor optical amplifiers (SOAs) [8] or microring resonators [9]. Nevertheless, these implementations showed some drawbacks, for instance, lack of flexibility of optical links, relative intensity noise (RIN) limitations and distortions of SOAs and narrowband behavior of microring resonators in terms of tuning speed.

To overcome those constraints, a novel technology approach able to integrate photonic TTDs in silicon platforms is proposed. This technology is based on the use of nanocomposites formed by the dispersion of colloidal quantum dots (QDs) in polymers [10]. This sort of multicomponent material is emerging as very suitable for many photonic applications, due to the combination of the QDs optical properties (room temperature emission and bandgap tunability) in addition to the technological properties of the polymers, i.e., deposition on films by different methods and patterning by UV or e-beam lithography. Following this interest, we have previously proposed to use the nanocomposites as cores of active waveguides able to provide MWP functions [10], [11], by exploiting the active properties of the QDs. As a first approach, we presented a planar waveguide structure fabricated by the dispersion of PbS QDs in Polymethyl methacrylate (PMMA) and the PS functionality studied [11]. In [12], we presented a second waveguide design consisting of a ridge bilayer structure composed by a QDs-SU8 core covered by a SU8 cladding to provide MWP PS behavior. However, in order to demonstrate a broadband, tunable and flexible MWP TTD unit based on those structures, a new study is provided in this letter. Therefore, this work is

focused on the practical demonstration of a continuous TTD capability by the proposed PbS-PMMA QDs and PbS-SU8 QDs waveguides over a broadband microwave frequency range. This paper first introduces the proposed photonic waveguide (PhW) structures and TTD characterization set-up. Then, it analyzes experimental time delay results and related amplitude signals in order to provide conclusion to outline further research.

## II. WAVEGUIDE FABRICATION

The samples used in this letter are based on nanocomposites fabricated by the dispersion of PbS QDs in a PMMA matrix and in a SU8 matrix. The resulting nanocomposite can act as the core of a waveguide whose active properties can be tuned by controlling the size, concentration and type of the embedded QDs [13]. Since the final goal is to demonstrate true-time delay by the absorption of these nanocrystals at optical telecommunication windows, i.e., 1550 nm, the size of the QD was fixed to be around 4.5 nm to show efficient absorption at these range of wavelengths [13]. In this particular case, absorption at 1550 nm can be saturated when the nanocrystals are pumped at 980 nm, because absorbance increases for short wavelengths, as depicted in Fig. 1. Then, saturation of the absorption of the QDs [14] is expected to vary the group index at 1550 nm and to produce a phase change on the traveling optical signals [15] and in consequence a temporal delay. In a first approach, the nanocomposite was fabricated by mixing the QD colloidal solution with PMMA with filling factor ( $ff$ ) of  $10^{-2}$  selected to obtain a compromise between field propagation waveguiding and QD excitation [10]. Then, it was deposited on a  $\text{SiO}_2/\text{Si}$  substrate (see Fig. 2 (a)) in order to be used as a core of an active planar waveguide.

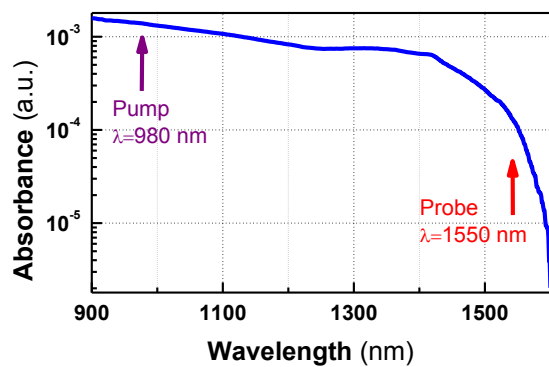


Fig. 1. Absorption value for to the pump (980 nm) and probe (1550 nm) wavelength of the PbS QD material for each PMMA and SU8 matrices, (a.u) is for absorbance units.

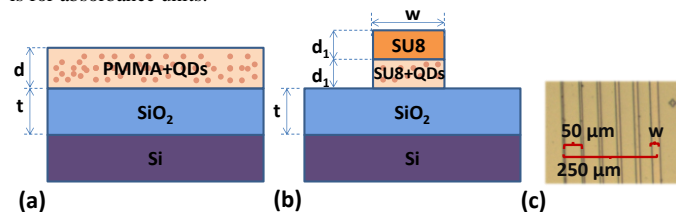


Fig. 2. Schematic view of the waveguides under study: (a) PbS-PMMA QDs and (b) PbS-SU8 QDs bilayer structures. (c) Snapshot of the upper view section of the PbS-SU8 QDs bilayer waveguide from optical microscope.

On the other hand, for the purpose of improving the flexibility of the MWP device, we proposed in [12] to pattern the nanocomposite by dispersing the PbS QDs on a SU8 matrix. A bidimensional ridge waveguide consisting of a bilayer structure composed by a SU8+QDs layer and a SU8 cladding incorporated to decrease the propagation losses was proposed, as shown in Fig. 2(b) and 2(c). The overall fabrication process is described in [12].

## III. TTD PRINCIPLE OF OPERATION & MEASUREMENT SET-UP

The working principle of the TTD device is based on the saturable absorption of the QDs when they are pumped below their bandgap. This effect will produce a phase change of the travelling optical signals and a temporal delay as discussed previously. In order to characterize the behavior of these integrated MWP QDs waveguides based on PMMA and SU8 as TTD units after photo-detection, the group index variation is translated into a phase change  $\Delta\varphi$  in the microwave signal, that can be expressed as:

$$\Delta\varphi = \Delta kL = \frac{\Omega}{c} \Delta n_g L, \quad (1)$$

being  $k$  the wave vector of the signal,  $c$  the speed of light in vacuum,  $\Omega$  the angular frequency of the RF tone,  $\Delta n_g$  and  $L$  the group index variation and the length of the medium, respectively. Then, the time delay value of the TTD for an instant bandwidth of 25 GHz ( $\Delta t$ ) is obtained as:

$$\Delta\varphi = -2\pi\Delta t \cdot \Delta f \rightarrow \Delta t = \frac{-\Delta\varphi}{2\pi\Delta f}, \quad (2)$$

where  $\Delta f$  is the operation frequency range where the delay is measured [16].

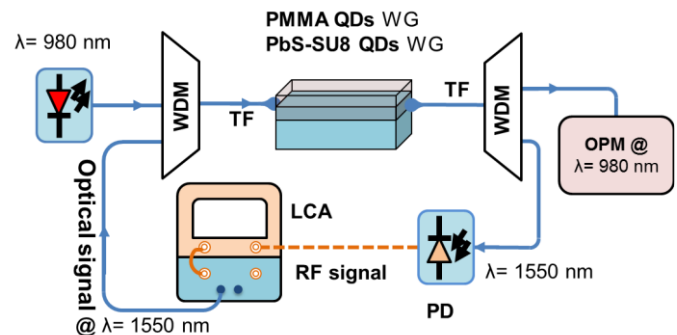


Fig. 3. Experimental laboratory set-up. LCA: light component analyzer; TF: tapered fiber tip; WG: waveguide and OPM: optical power meter, PD: photodetector.

The set-up used is shown in Fig. 3. A microwave tone (10 MHz - 25 GHz) generated by a vector network analyzer (VNA), as part of a light component analyzer (LCA) is used to electro-optically modulate the continuous-wave (CW) laser at 1550 nm. Then, the double side band optical signal is mixed at a wavelength division multiplexer (WDM) with a 980 nm CW pump laser, once a time for each sample. The two beams that are mixed at the output of the WDM are injected into the waveguide thanks to a tapered fiber (TF) [17]. At the output edge of the waveguide, light is collected with another tapered fiber and pumped into a WDM in order to separate the 1550 and 980 nm signals. The 980 nm optical signal is measured by

and optical power meter (OPM) only for calibration purposes. The 1550 nm signal is electrically converted by a photodetector (PD) and injected to the RF port of the LCA where its magnitude and phase are measured.

#### IV. EXPERIMENTAL RESULTS

Photonic waveguide samples were tested as TTD units by characterizing the microwave signal with the set-up explained in section III. Temporal delay suffered by the RF signal along its entire bandwidth (10 MHz - 25 GHz) was calculated by increasing the pump power at 980 nm progressively, while the power of the signal at 1550 nm wave was kept constant.

##### A. PMMA waveguide TTD results

The PbS-PMMA planar waveguide under study was pumped at 980 nm as explained in section III. The waveguide length was set to 4 mm, while the nanocomposite and PMMA cladding thicknesses were  $t = 2 \mu\text{m}$  and  $d = 3 \mu\text{m}$ , respectively, to ensure signal propagation. In this set-up the total optical loss was 33 dB, comprising 10 dB due to TF light coupling, 19 dB/cm propagation losses for the PMMA QDs PhW sample and set-up experimental losses. The time delay performed by the excitation of the QD PbS at the pumping wavelength of 980 nm has been studied and analyzed. The results are shown in Fig. 4 and Fig. 5.

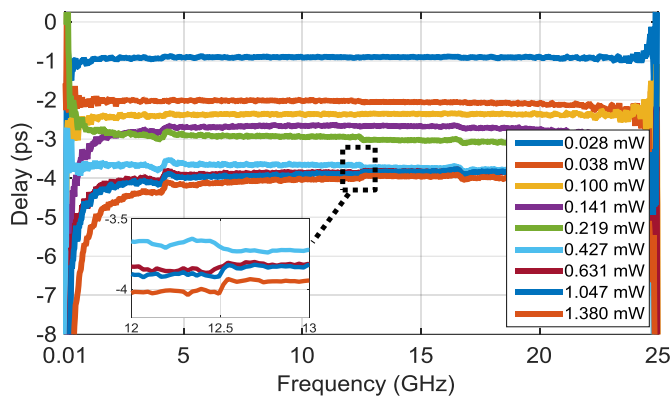


Fig. 4. Time delay as a function of the microwave frequency for different 980 nm pump powers in the 4 mm long PbS-PMMA QDs waveguide.

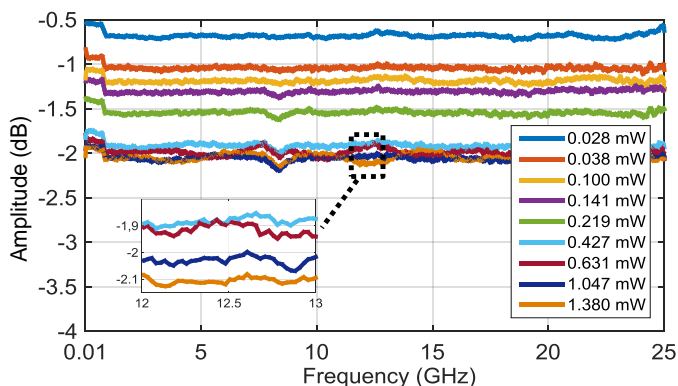


Fig. 5. Normalized amplitude response as a function of the microwave frequency in the 4 mm long PbS-PMMA QDs waveguide.

The results presented in Fig. 4 indicate that the higher the pump power the larger the time delay, saturating to values up to 4 ps, probably due to nanocrystal saturation [18]. Note that

the variations in RF amplitude are less than 2 dB, as illustrated in Fig. 5. In both graphs it is interesting to observe that for pumping powers above 0.6 mW, the amplitude and delay values reach a stable regime due to the saturation of the QDs absorption. The irregularity peaks observed in the measurements, lower than  $\pm 0.1$  ps and  $\pm 0.1$  dB, are not caused by the TTD operation principle. In fact, they are attributed to the IF bandwidths at the LCA used. These results prove the feasibility to tune continuously a broadband TTD with the proposed PbS-PMMA QDs waveguide.

##### B. SU8 bilayer waveguide TTD results

For the proposed PbS-SU8 QDs bilayer structure, different waveguides widths and lengths were tested. In this case, as demonstrated previously as phase shifters [12], the narrower/longer the waveguide the higher the phase shift/time delay produced. The best results, showed in Fig. 6, were produced by the 4  $\mu\text{m}$  thick (thickness of the  $\text{SiO}_2/\text{Si}$  substrate  $t = 4 \mu\text{m}$  and of the SU8/SU8+QDs cladding  $d_l = 2 \mu\text{m}$ ), 20  $\mu\text{m}$  wide ( $w$ ), 6 mm long and  $ff=10^{-2}$ , ensuring signal propagation. In this set-up, the total optical loss was 22 dB, comprising 10 dB due to TF light coupling and 6 dB/cm propagation losses for the PbS-SU8 QDs PhW and set-up experimental losses.

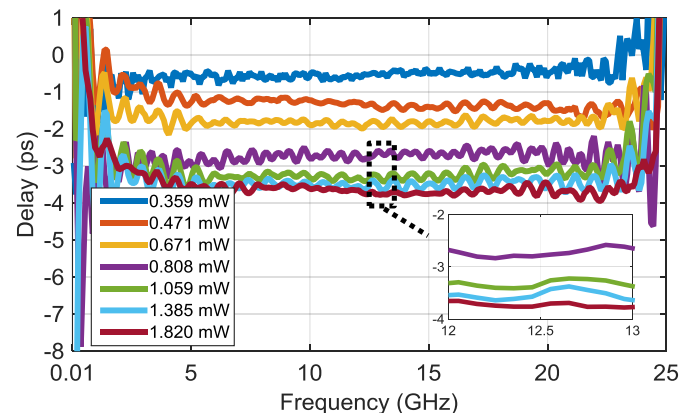


Fig. 6. Time delay as a function of the microwave frequency for different 980 nm pump powers in the 20  $\mu\text{m}$  wide and 6 mm long PbS-SU8-QDs bilayer waveguide.

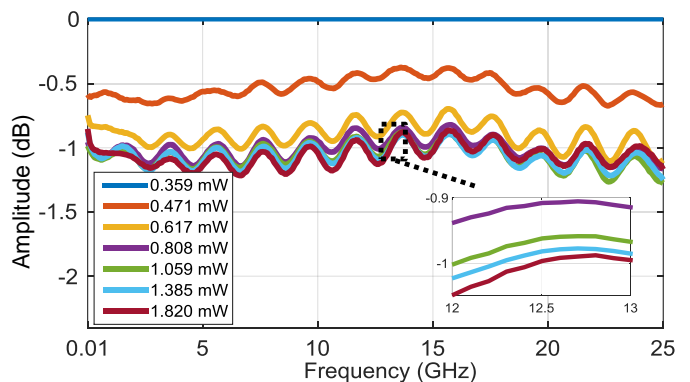


Fig. 7. Normalized amplitude response as a function of the microwave frequency in the 20  $\mu\text{m}$  wide 6 mm long PbS-SU8 QDs bilayer waveguide.

Again, the higher pump power, the larger time delay as shown in Fig. 6. The inset in Fig. 6 indicates that for pump power values beyond 1.05 mW, a saturation level at the nanocrystal is obtained. Fig. 7 shows the normalized detected



signal power for different coupled pump powers. The graph showed a saturation level for the receiving signal, as previously discussed. This regime is due to the fact that the SU8 waveguide has a finite number of QDs and their excitation reaches a saturation regime of absorption [18]. The small amplitude variation in Fig. 7 is due to the size of the TF light spot at the edge of the waveguide that is slightly bigger than the thickness ( $d_1$ ) of the single SU8-QDs cladding. Therefore, light is propagated and confined in both claddings.

Clearly, PMMA and SU8 waveguides have been proved as potential photonic TTD units with more than 3.5 ps continuous temporal delay over more than 25 GHz range. This frequency range and the tuning speed are limited by the RF measurement set-up, not by the different waveguides structures. In this letter, both waveguides samples were selected to increase the temporal delay with a similar width and length. However, the SU8 bilayer waveguide structure allows confining the light better and therefore to control more properly the delay functionality due to higher light excitation of the QDs. The results indicate that it improves the range of pump power absorption of the QDs due to its structure, as showed in Fig. 6 and Fig. 7. In addition, the novel structure of the SU8 bilayer waveguide compared with the PMMA waveguide adds the SU8 cladding waveguide width parameter  $w$  as a new flexibility level of design for future on-chip requirements, e.g., PICs width matching. Moreover, the bilayer SU8 waveguide shows a bigger SNR than the PMMA due to smaller optical power losses, as can be seen by comparing Fig. 5 and Fig. 7.

The temporal delay value obtained could be improved by modifying the design of the sample to obtain an enhanced confinement of the light and a better excitation of the QDs. As example, the increment of the pump conditions with a novel characterization set-up with a dual light pumping from either edges or a surface light pumping directly to the excitation area will improve light confinement and nanostructure excitation. On the other hand, novel structures with higher QDs concentration that will improve the excitation area [19] could be considered for further research.

## V. CONCLUSIONS

In this work, a novel approach to implement MWP TTD unit devices based on PbS-PMMA and PbS-SU8 nanocomposites with QDs integrated into silicon platforms is reported. The results obtained prove that both structures are able to perform a real time MWP TTD function of more than 3 ps over a broadband 25 GHz RF range for 1550 nm optical telecommunications signals. The PbS-SU8 bilayer waveguide shows potential design advantages over the PbS-PMMA waveguide due to a better light confinement. This work demonstrated a continuous and fast true-time delay tunability under broadband RF operation with the proposed SU8-QDs and PMMA-QDs structures. These PhW structures could be designed to face future on-chip requirements and being considered as effective photonic TTD units.

## ACKNOWLEDGMENTS

The authors would like to thank Prof Antonio Díez (Semiconductor and Fiber Optics group from the University of Valencia) for the fabrication of the tapered fiber tip and Dr Pedro J. Rodríguez Cantó and Dr Rafael Abargues (Intenanomat S.L, Valencia, Spain) for their fruitful discussions about nanocomposites and quantum dots.

## REFERENCES

- [1] J. Capmany and D. Novak, "Microwave photonics combines two worlds," *Nat Phot.*, vol. 1, no. 6, pp. 319–330, 2007.
- [2] A. J. Seeds and K. J. Williams, "Microwave Photonics," *J. Light. Technol.*, vol. 24, no. 12, pp. 4628–4641, Dec. 2006.
- [3] J. Capmany, I. Gasulla, and D. Perez, "Microwave photonics: The programmable processor," *Nat Phot.*, vol. 10, no. 1, pp. 6–8, Jan. 2016.
- [4] J. Yao, "Microwave Photonics," *J. Light. Technol.*, vol. 27, no. 3, pp. 314–335, Jan. 2009.
- [5] J. Capmany, J. Mora, I. Gasulla, J. Sancho, J. Lloret, and S. Sales, "Microwave Photonic Signal Processing," *J. Light. Technol.*, vol. 31, no. 4, pp. 571–586, 2013.
- [6] D. Marpaung, C. Roeloffzen, R. Heideman, A. Leinse, S. Sales, and J. Capmany, "Integrated microwave photonics," *Laser Photon. Rev.*, vol. 7, no. 4, pp. 506–538, 2013.
- [7] E. Udvary and T. Berceli, "New microwave / millimeter wave true time delay device utilizing photonic approaches," *Microw. Conf. (EuMC), 2010 Eur.*, pp. 121–124, 2010.
- [8] Y. Minamoto and M. Matsuura, "True-time delay beamforming using semiconductor optical amplifier and tunable dispersion medium," in *2014 4th IEEE International Conference on Network Infrastructure and Digital Content*, 2014, pp. 164–167.
- [9] J. Cardenas, S. Manipatruni, N. Sherwood-Droz, C. B. Poitras, B. Zhang, J. B. Khurgin, P. A. Morton, and M. Lipson, "Large Tunable Delay of an RF Photonic Signal with 130 GHz Bandwidth Using Silicon Microresonators," in *Conference on Lasers and Electro-Optics 2010*, 2010, p. CWG3.
- [10] I. Suárez, H. Gordillo, R. Abargues, S. Albert, and J. Martínez-Pastor, "Photoluminescence waveguiding in CdSe and CdTe QDs-PMMA nanocomposite films," *Nanotechnology*, vol. 22, no. 43, p. 435202, 2011.
- [11] A. L. Ricchiuti, I. Suarez, D. Barrera, P. J. Rodriguez-Canto, C. R. Fernandez-Pousa, R. Abargues, S. Sales, J. Martinez-Pastor, and J. Capmany, "Colloidal Quantum Dots-PMMA Waveguides as Integrable Microwave Photonic Phase Shifters," *Photonics Technol. Lett. IEEE*, vol. 26, no. 4, pp. 402–404, 2014.
- [12] J. Hervás, I. Suárez, J. Pérez, P. J. R. Cantó, R. Abargues, J. P. Martínez-Pastor, S. Sales, and J. Capmany, "MWP phase shifters integrated in PbS-SU8 waveguides," *Opt. Express*, vol. 23, no. 11, pp. 14351–14359, 2015.
- [13] H. Gordillo, I. Suárez, R. Abargues, P. Rodríguez-Cantó, S. Albert, and J. P. Martínez-Pastor, "Polymer/QDs nanocomposites for waveguiding applications," *J. Nanomater.*, vol. 2012, p. 33, 2012.
- [14] M. Corp., "MicroChem SU-8 Negative Epoxy Series Resists." [Online]. Available: [http://www.microchem.com/Prod-SU8\\_KMPR.htm](http://www.microchem.com/Prod-SU8_KMPR.htm). [Accessed: 14-Dec-2015].
- [15] W. Xue, S. Sales, J. Capmany, and J. Mørk, "Wideband 360 microwave photonic phase shifter based on slow light in semiconductor optical amplifiers," *Opt. Express*, vol. 18, no. 6, pp. 6156–6163, 2010.
- [16] R. Bonjour, S. A. Gebrewold, D. Hillerkuss, C. Hafner, and J. Leuthold, "Continuously tunable true-time delays with ultra-low settling time," *Opt. Express*, vol. 23, no. 5, pp. 6952–64, Mar. 2015.
- [17] L. Arques, A. Carrascosa, V. Zamora, A. Díez, J. L. Cruz, and M. V. Andrés, "Excitation and interrogation of whispering-gallery modes in optical microresonators using a single fused-tapered fiber tip," *Opt. Lett.*, vol. 36, no. 17, pp. 3452–3454, 2011.
- [18] V. I. Klimov, S. A. Ivanov, J. Nanda, M. Achermann, I. Bezel, J. A. McGuire, and A. Piryatinski, "Single-exciton optical gain in semiconductor nanocrystals," *Nature*, vol. 447, no. 7143, pp. 441–6, May 2007.
- [19] I. Suárez, A. Larrue, P. J. Rodríguez-Cantó, G. Almuneau, R. Abargues, V. S. Chirvony, and J. P. Martínez-Pastor, "Efficient excitation of photoluminescence in a two-dimensional waveguide consisting of a quantum dot-polymer sandwich-type structure," *Opt. Lett.*, vol. 39, no. 16, pp. 4962–4965, 2014.